J. Electrochem. Sci. Eng. **15(5)** (2025) 2705; http://dx.doi.org/10.5599/jese.2705

Open Access : : ISSN 1847-9286
www.jESE-online.org

Original scientific paper

Covalent attachment of aminoferrocene to pseudo-graphite for selective sensing of H_2O_2

Forrest Dalbec[1], Jeremy May[1], Dipak Koirala[1], Jhonnathan A. Plascencia[1], Micheal Okeke[1], Joshua A. Russell[2], Hui Xiong[2] and I. Francis Cheng[1,✉]

[1]*Department of Chemistry, University of Idaho, 875 Perimeter Dr, Moscow, ID-83844, USA*
[2]*Micron School of Materials Science and Engineering Boise State University Boise ID 83725, USA*

Corresponding author: ✉*ifcheng@uidaho.edu*

Received: March 10, 2025; Accepted: June 4, 2025; Published: July 9, 2025

Abstract

Hydrogen peroxide is an important analyte from both the standpoints of in vivo and in vitro analyses. Electrochemical methods offer good prospects, but present sensing methods suffer from inadequate limits of detection (LOD), low sensitivity, poor stability, and numerous interferents. To address these issues, we use the recently recognized peroxidase-like activity of ferrocene for sensing based on the reductive electrocatalysis of H_2O_2. This route obviates interferences from ascorbate, urea, urate, dopamine and glucose. Immobilization of ferrocene overcomes its low aqueous solubility. This is done by the chemical modification of a pseudo-graphite material rich in sp^3 defects. The surface is modified for carboxylate features through a diazonium intermediate formed through 4-aminobenzoic acid. Aminoferrocene is attached to surface carboxylate groups through a N-ethyl-N'-(3-(dimethylamino)propyl) carbodiimide coupling agent. Cyclic voltametric studies indicate that the surface concentration of ferrocene is 1.06 nmol cm^{-2}. Chronoamperometric response at -0.6 V vs. Ag/AgCl, gives a LOD of 0.070 µM with a high sensitivity of 553.2 µA mM^{-1} cm^{-2}. This is the best sensitivity reported in the literature. Furthermore, the sensor is stable over 50 cyclic voltametric scans, and between the 3 calibration-curve studies.

Keywords

Peroxide detection; ferrocene; interference-free; diazonium; graphitic carbon

Introduction

Hydrogen peroxide is an important medical biomarker as an increase in peroxide concentration in biofluids is associated with diseases such as diabetes and cancer [1,2]. In these biological matrices, the concentration of H_2O_2 can range from 0.1 to 100 µM [1,2]. Increases in peroxide concentration as small as 0.1 µM can indicate malignant cells, and thus, sensitive methods for detection are highly desired. Electrochemical methods are one option as they offer rapid and sensitive analysis, with the further possibility of *in situ* sensors. Electrochemical detection for H_2O_2 proceeds through peroxide

oxidation (Equation 1) or reduction (Equation 2) and can be performed using various electrode materials [3,4].

$H_2O_2 = O_2 + 2e^- + 2H^+$ $E^{0\prime}(1) = +0.695V$ (1)

$H_2O_2 + 2H^+ + 2e^- = 2\ H_2O$ $E^{0\prime}(2) = +1.763V$ (2)

However, these electrodes generally suffer from either slow kinetics, instability, a modest limit of detection (LOD) or matrix interferences [5,6] . Therefore, electrocatalysts are often required for H_2O_2 sensing, with the predominant one being horseradish peroxidases (HRP) [4]. This enzyme contains an electrocatalytic heme moiety, which oxidizes peroxide (Equation 1), but its surrounding protein shell prohibits direct electroreduction and requires a redox mediator for peroxide detection [4-6]. Sensors based on HRP generally have an excellent LOD of up to 10^{-7} M with linear ranges of 1 to 2 orders of magnitude. However, their reliance on redox mediation causes an increased susceptibility to electrochemically active biological interferents. Furthermore, the enzyme itself is degraded by hydrogen peroxide, which limits the electrocatalytic turnover number and durability [3,5,6]. Due to these concerns, recent attention has been paid to alternative electrocatalysts.

However, all electrocatalysts still face interference from electroactive biomolecules. These include glucose (5.5 mM), ascorbate (100 mM), urea (7 mM), uric acid (0.4 mM), dopamine (200 pM) and in some instances, dissolved oxygen [7-11]. All these species, besides dissolved oxygen, can be electrochemically oxidized and therefore interfere with the electro-oxidative process of Reaction 1. Analysis of H_2O_2 by electro-reduction (Reaction 2) obviates most of these interferences except for dissolved O_2. This interference arises from the oxygen reduction reaction (ORR), Equation (3).

$O_2 + 4H^+ + 4e^- = 2H_2O$ $E^0 = 1.23$ V (3)

Normally, in biofluids, the concentrations of ascorbate and urate are high enough to completely remove dissolved oxygen from the sample (C_{O_2} = 0.13 mM at room temperature) [12,13]. However, prolonged exposure *ex situ* may include this interferent. Sulphite offers a possibility of removing $O_{2(aq)}$ from these samples through Equation (4) [14].

$SO_3^{2-} + ½\ O_2 = SO_4^{2-}$ (4)

Ferrocene (Fc) has recently been recognized as having many possible catalytic and electrocatalytic properties [15]. Among these include peroxidase-like activity, which may enable the catalysis of Reaction 2 or other electro-reductive reactions for the purpose of H_2O_2 sensing [16]. Ferrocene/ /ferricenium (Fc^+) redox couple has fast heterogeneous electron transfer with most electrodes and can charge mediation with dissolved species. Limitations include very low solubility in water and decomposition of Fc^+ by hydrolysis [17,18]. Immobilization of Fc on the electrode overcomes these issues [17,18]. In contrast to redox polymers, direct covalent attachment of Fc places it near the electrode surface [19]. This facilitates fast heterogenous electron transfer [19]. However, present methods of covalent attachment do not give stability, nor the surface concentration required for sensitive and robust sensing of H_2O_2 [20-22]. In this study, Fc is covalently attached to a pseudo-graphite. Graphite from the University of Idaho Thermalized Asphalt Reaction (GUITAR) consists of 85 % sp^2 and 15 % sp^3 C with a very small crystallite grain size of 1.5 nm [23]. This results in a high degree of basal plane defects, as shown in Figure 1. These defects allow for functionalization to a greater extent than defect-free graphites and graphenes [24,25]. The network of six-membered ring systems of the latter two gives a stabilized surface that is difficult to modify [26-28]. Furthermore, functionalization of the defects on GUITAR does not negatively affect the materials stability [29-31]. In a recent contribution, this was demonstrated by the stable covalent attachment of single-strand DNA to GUITAR for molecular recognition [29]. This is the only known attachment that is able to

withstand the temperatures required for the polymerase chain reaction [29]. In this contribution, spontaneous diazonium addition and sequential amide bond coupling was used for the immobilization of Fc (see Figure 2, below) [29]. We evaluate this modified GUITAR for performance for H_2O_2 detection in the presence of common interfering agents.

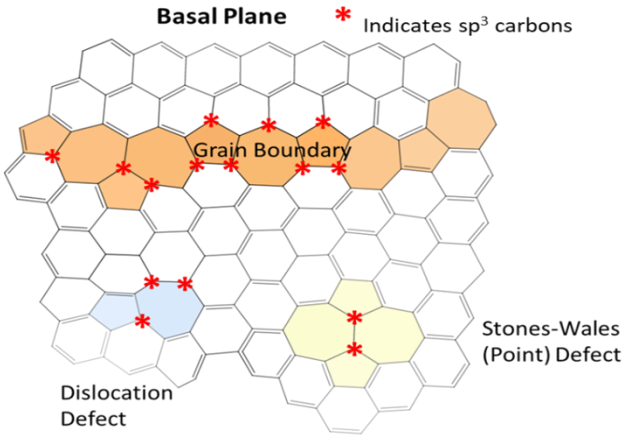

Figure 1. *The various structural defects within the basal plane of graphite. These defects give GUITAR its chemically functionalizable surface at the sp^3-like sites*

Adding to the impetus of using GUITAR is its excellent electrode characteristics. These include fast heterogeneous electron transfer, a wide aqueous potential window and resistance to fouling [23,30,31]. These qualities make it an excellent material for electrochemical sensing.

Experimental

Chemicals

Vegetable oil (WinCo brand) was obtained at a WinCo Foods grocery store (Moscow, ID, USA). Carbon black (CB, acetylene, 50 % compressed, 99.9 %) was obtained from Alfa Aesar (Ward Hill, Massachusetts). 4-aminobenzoic acid (99 %), 1-ethyl-3-[3-dimethyl aminopropyl] carbodiimide (EDC) (≥97 %), and 2-(N-morpholino)ethanesulfonic acid (MES) (≥99.5 %) were obtained from Sigma Aldrich (St. Louis, MO, USA). Hydrochloric acid (36.5 to 38 % w/v), sodium hydroxide (98.9 %), magnesium chloride (99 %), and sodium nitrite (98 %), potassium monophosphate (99.6 %), potassium diphosphate (99.8 %), sodium oxalate, Fischer Primary Standard and potassium chloride (99.7 %) were obtained from Fisher Scientific (Waltham, NJ, USA). Potassium ferricyanide was obtained from Acros Organics (N.J, USA). 5 % Nafion solution dispersion (D521) was obtained from Ion Power Inc. (Tyrone, PA, USA). Hydrogen peroxide solution 30 %, AR® ACS, was obtained from Macron Fine Chemicals (Center Valley, Pennsylvania, USA). The 30 % hydrogen peroxide solution was standardized weekly against a secondary standard potassium permanganate. Potassium permanganate (≥99.0 %), BAKER ANALYZED® ACS, was obtained from Avantor Performance Material LLC (Center Valley, Pennsylvania, USA). Potassium permanganate was standardized daily against the primary standard sodium oxalate. All aqueous solutions were prepared with deionized water purified by passage through an activated carbon purification cartridge obtained from Barnstead - model D8922 (IA, USA).

Chemical vapor deposition of GUITAR on carbon black particles

GUITAR particles were formed by chemical vapor deposition (CVD) onto carbon black (CB) particles as described in detail in previous publications [31,32]. In summary, the vegetable oil precursor was injected into a 900 °C quartz tube furnace containing the CB substrate under an inert (N_2) atmosphere

for 15 min. Three successive coating cycles were performed, with the coated particles being passed through an 80-micron mesh screen between cycles.

Coupling of aminoferrocene to GUITAR surfaces

Ferrocene attachment of GUITAR particles is highlighted in Figure 2. The following were added to 80 mL of water at 0-5 °C: 280 mg NaOH, 526 mg $NaNO_2$ and 960 mg 4-aminbenzoic acid [29]. This solution was slowly acidified to pH 2, generating 4-carboxybenzoicdiazonium (i) in Figure 2. After 45 minutes, 200 mg of GUITAR particles were added to the mixture and allowed to react for 2 hours. Carboxylated GUITAR particles were filtered and washed with deionized water and isopropyl alcohol. Carboxylated GUITAR particles (20 mg) were added to 1.0 mL of 50/50 (v/v) water/ethanol solution containing 0.1 M MES buffer at pH 4.5. To this, 100 µL of 1.3 M EDC and 100 µL of 10 mM aminoferrocene were slowly added. The solution was vigorously stirred for 16 hours at room temperature. The particles were decanted and washed 3 times with absolute ethanol, acetone, and DI water, respectively.

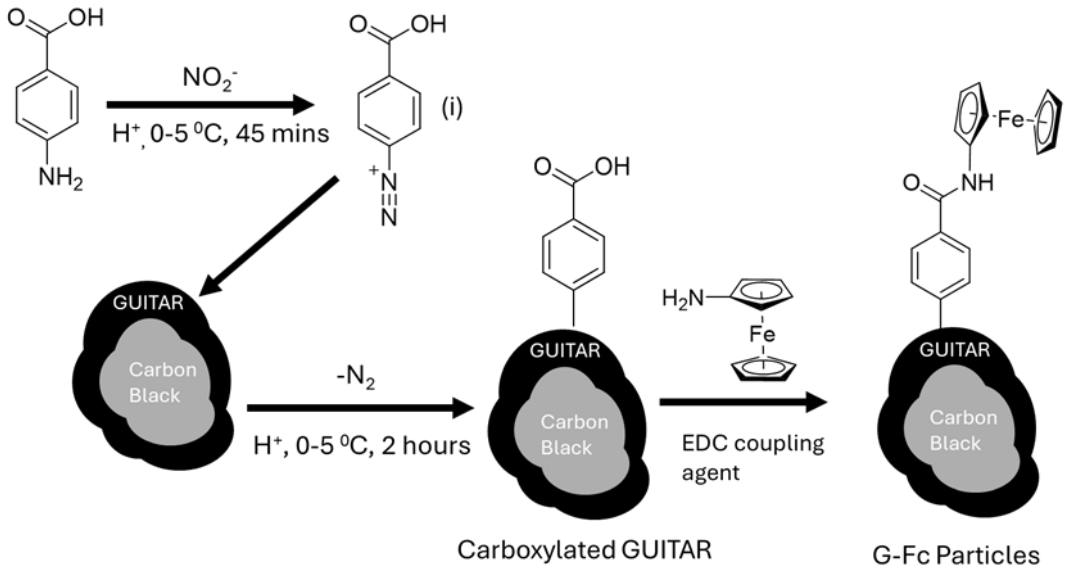

Figure 2. *Schematic for the immobilization of ferrocene onto GUITAR particles. This process was also performed on carbon black, which served as a control*

Electrode ink fabrication and electrochemical setup

For electrochemical experiments, particles were cast onto a glassy carbon substrate as Nafion thin-film inks as previously described [31,32]. In short, inks were made with 20 mg of particles in 1 mL total volume, consisting of 450 µL of ethanol, 450 µL of DI H_2O, and 150 µL of 5 % Nafion solution. The particle loading of CB was ~1.0 mg cm^{-2}, which is the same as in our previous studies [31,32]. Cyclic voltametric (CV) electrochemical studies were performed with a Bioanalytical Systems CV-50 W (West Lafayette, IN, USA). In all cases, these studies used an Ag/AgCl reference electrode (3.0 M KCl, 0.209 V *vs*. SHE) and a graphite rod as the counter electrode in an undivided cell. Electrochemically active surface area (ECSA) was determined on GUITAR by measuring the CV capacitance currents described in previous publications [23,31,32]. The geometric surface area was used for CB electrodes.

X-ray photoelectron spectroscopy characterization

X-ray photoelectron spectroscopy (XPS) was performed on a Physical Electronics PHI5600 spectrometer (Chanhassen, Minnesota, USA). Measurements were made with the Al Kα emission

line (1486.6 eV) and a hemispherical energy analyzer with a resolution of 0.025 eV. Samples were grounded and exposed to a 500-eV electron beam to eliminate spurious charging. All spectra were acquired at room temperature. The XPS peaks were fitted with associated Gaussian-Lorentzian curves on XPSPEAK41 in accordance with the graphitic materials literature [33-37]. Tougaard background subtraction was performed for peak deconvolutions [33-37]. The full widths at half maximums (FWHM) were held at a constant value for all peaks during deconvolution.

Results and discussion

XPS of carboxylate GUITAR particles

Wide-scan XPS of (Figure 3A) revealed two peaks assigned to C1s at 285 eV and O1s at 532 eV. Using Tougaard background subtraction, and the surface relative sensitivity factors from Wagner, the oxygen content is 14.9 at.% [35-38]. This corresponds to 7.5 at.% -COOH groups on the surface relative to C abundance. This is the highest surface coverage for chemical diazonium grafting presented in the literature [39-47]. Also, this conclusion is supported by the deconvolved C1s peak (displayed in Figure 3B), which gives 38.8 at.% sp^2 C at 284.5 eV, 35.9 at.% sp^3 C at 285.1 eV, 13.5 at.% -C=O at 286.7 eV and 8.1 at.% -COOH at 288.7 eV [34-38].

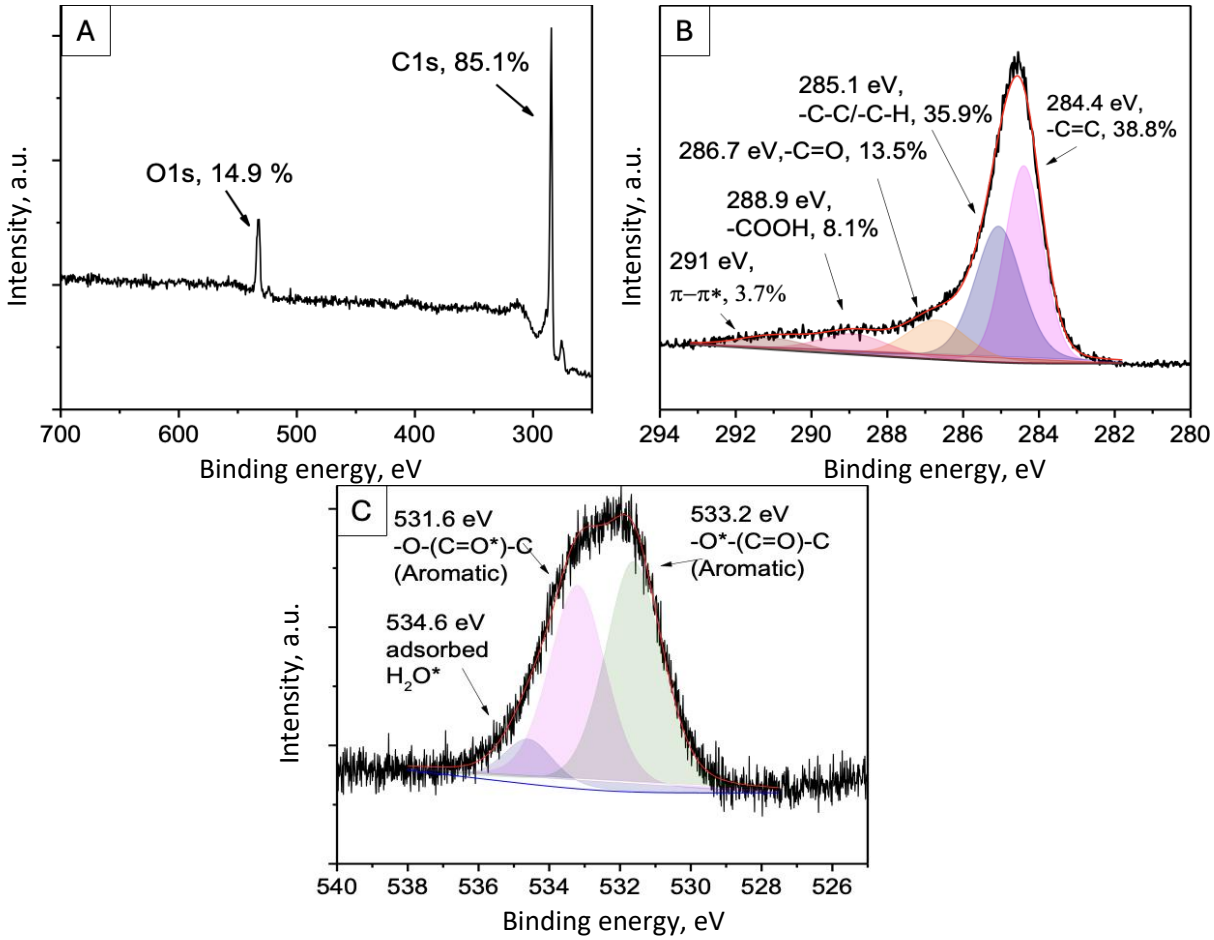

Figure 3. *XPS analysis of diazonium grafted particles of GUITAR-COOH. (A) Survey scan spectrum of GUITAR-COOH with relative atomic abundances. The C1s (B), and O1s (C) are displayed with associated deconvolved peaks*

The O1s peak (Figure 3C) reveals three deconvolved oxygen peaks, at 531.6 eV corresponding to -C=O, 533.2 eV for -C-O. The last at 534.6 eV is attributed to adsorbed water [34-36,38,48,49]. Adventitious carbon is a concern in XPS analysis, this species is primarily from ambient volatile

organic carbons (VOCs) [50]. This possibility was discounted as VOCs if the O peak in the survey scan is absent. VOCs average 25/75 O/C ratio, also the C-C peak for VOCs are at 284.8 +/-0.25 eV, which is absent in our XPS scans [50]. A common but detrimental side product is incomplete reduction of diazonium salt, leaving residual -N=N on the surface [39-47,51-53]. This was considered negligible as no N1s peaks were observed in the survey scan [35,38,48,53]. It is important to note that attachments of diazonium salts to the BP of graphitic materials are weaker than true covalent bonds, as observed by Lim and coworkers [24]. The high yield achieved on GUITAR is likely due to the high defect density observed on the basal plane, which can more readily react with the diazonium salts formed in solution [24,25].

XPS analysis of immobilized ferrocene

Surface-bound ferrocene was attached through an amide linkage as outlined in Figure 2, Step 2. XPS studies of GUITAR-Fc particles yield an average iron content of 2.55 at.%. The peak assignments and relative atomic abundances from the survey XPS are shown in Figure 4A. The visibility of the Fe2s peak was also present in the survey scan presented in Figure 4A. This is not seen with literature XPS ferrocene and may indicate that the core electronic levels of the ferrocene have been affected by covalent linkage to GUITAR. As discussed above, the relative carboxylate content on GUITAR is 7.47 at %. Comparing the two relative quantities gives a yield of 34 % (2.55/7.47 at.%) of attached ferrocene relative to carboxylate.

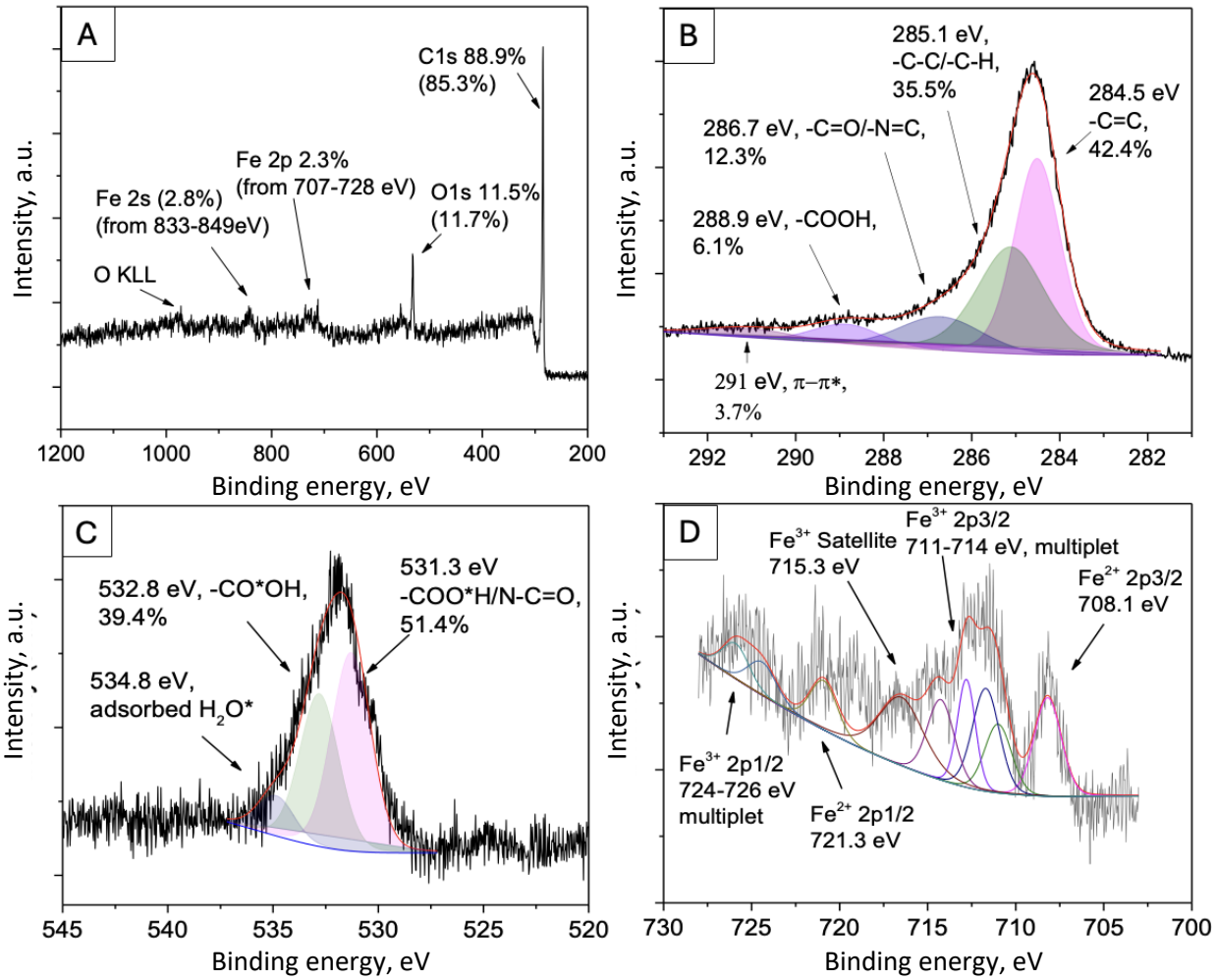

Figure 4. XPS analysis of GUITAR-Fc. (A) Survey scan spectrum of with relative atomic abundances. Values presented in parenthesis are at.% using Fe2s peak. The C1s (B), O1s (C), and Fe2p (D), high-resolution scans are displayed with associated deconvolution

In literature, ferrocene coupling reactions with diazonium modified surfaces only proceed to about 10 % yield [51-53]. The detailed scan of the Fe2p region is presented in Figure 4D. While the scan appears to have features of ferrocene present in literature, no conclusions can be drawn with any confidence, as the scan quality is low.

Electrochemical characterization of immobilized ferrocene

Immobilized ferrocene on GUITAR and CB particle film electrodes was examined with cyclic voltammetry (CV). Both surfaces were modified by the sequence outlined in Figure 2. Figures 5A and 5B show the cyclic voltammograms of GUITAR-Fc and CB-Fc, respectively, at a scan rate of 0.05 V s^{-1} in 0.1 M phosphate buffer (PB) at pH 7.0 under atmospheric conditions. The background CVs consist of associated carboxylated particles without ferrocene.

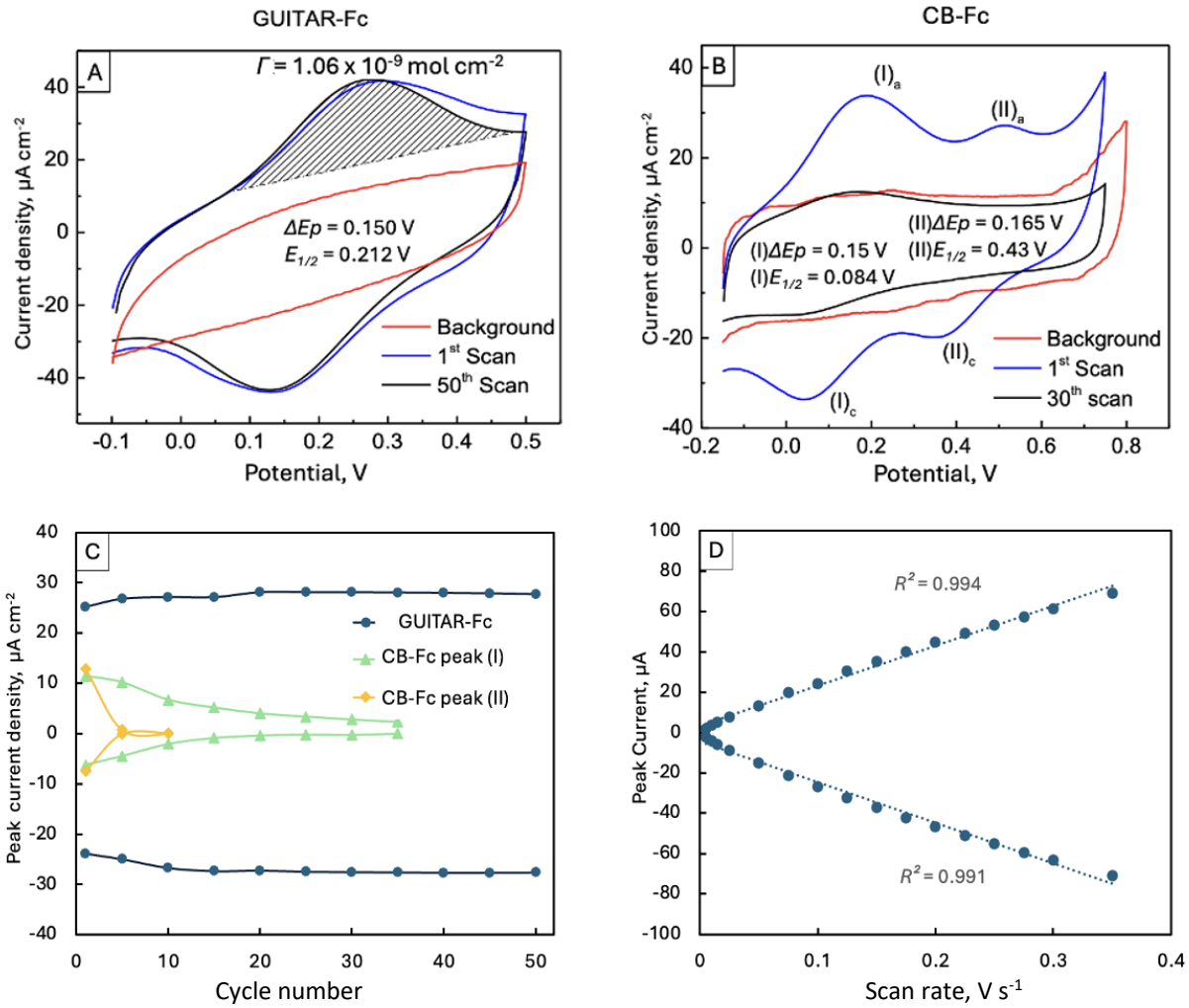

Figure 5. *(A) CV scans (0.05 V s^{-1}) on GUITAR-Fc (1st - blue line, 50th- black line) and GUITAR-COOH (red line). (B) CV scans CB-Fc (1st - blue line, 30th- black line) and CB-COOH (red line). (C) The peak current densities for both materials over respective CV cycles. GUITAR-Fc shows no loss in peak current over 50 cycles whereas CB-Fc loses all its peak current density within 30 cycles. (D) A plot of scan rate vs. peak current, there is a linear correlation between these variables showing that Fc exhibits adsorbed species*

Figure 5A shows a reversible pair of redox peaks on GUITAR-Fc attributed to the $1e^-$ ferrocene/ferrocenium (Fc/Fc^+) redox couple. On GUITAR, it has a ΔE_p of 150 mV, an $E_{1/2}$ of 212 mV *vs*. Ag/AgCl, and a stable I_{pa}/I_{pc} ratio of 1.05 (peak current anodic I_{pa} over peak current cathodic I_{pc}) over 50 CVs. The i_ps had a linear dependence on scan rate, showing the Fc on GUITAR had adsorbed species (Figure 5D) [13,54]. The CB-Fc CVs in Figure 5B show two sets of CV waves, both degrading

to background in less than 30 CV scans. This indicates that the diazonium coupling scheme in Figure 2 was not as successful with CB. Additionally, a portion of aminoferrocene was weakly adsorbed onto that surface.

The surface coverage (Γ) of Fc on GUITAR was determined by integration of the anodic CV wave (shaded region, Figure 5A) and equation (5) below [13,54].

$$\Gamma = \frac{Q}{nFA} \tag{5}$$

The symbol *Q* is the total amount of charge from that integration, *n* is the number of electrons transferred in the redox event, *F* is Faraday's constant, and *A* / cm^2 is the ECSA of the electrode. The calculated surface coverage is 1.06 nmol cm^{-2}. This compares well to other Fc covalent attachment schemes, which average 0.10 to 1.00 nmol cm^{-2} [20,55]**.**

Hydrogen peroxide detection with GUITAR-Fc electrodes

To assess the characteristics for electrochemical sensing of H_2O_2 by GUITAR-Fc, a CV wave at 50 mV/s was obtained under Ar-purged conditions in 0.1 M phosphate buffer (PB) at pH 7.0. A reductive current for 60 µM H_2O_2 is observed with an onset potential of -0.35 V (Figure 6A). Control particles without immobilized Fc showed no faradaic features up to 6612 µM H_2O_2. These results indicate the electrocatalytic role of Fc in this sensor. The chronoamperometric response for concentrations of H_2O_2 varying from 0.45 to 74 µM was obtained at -0.6 V *vs.* Ag/AgCl in Figure 6B. The limit of detection (LOD) of 0.34 µM was calculated using equation (6) below:

$$\text{LOD} = \frac{3.3\sigma}{m} \tag{6}$$

where σ is the standard deviation (0.062 µA cm^{-2}) of the seven replicates' lowest concentration signal in this study, 0.999 µM. Both the European Federation of Clinical Chemistry and Laboratory Medicine (EFLM) and IUPAC definitions for LOD use the standard deviation of the blank (σblank = 0.012 µA cm^{-2}, *n* = 15) [56-58]. Using this, the LOD is 0.070 µM. The slope of the responses for H_2O_2 detection in Figure 6D is 553.2 µA M^{-1} cm^{-2}. High sensitivity is desired as peroxide concentrations between a healthy and diseased cell are as low as 0.1 µM [1-3]. This is the highest reported sensitivity for a ferrocene-based system. Table 1 summarizes the linear ranges, sensitivities, and LOD for electrochemical detection of H_2O_2 from the literature and this study.

In addition to performance, GUITAR-Fc also demonstrates good sensor stability. Figure 6D demonstrates this, as the slopes and amperometric responses were identical over 3 calibration runs with a single electrode. In contrast, the CB-Fc control saw nearly complete loss of ferrocene/ /ferrocenium activity after only a single calibration run. Additionally, GUITAR-Fc shows excellent stability during long-term storage. The initial batch of GUITAR-Fc used in this study was stored for the duration of 1.5 years at 4 °C before use. A freshly prepared batch of GUITAR-Fc was used for replicates, and the same current responses and sensitivities were produced as the stored batch. This indicates no degradation of performance due to long-term storage. This is a distinct advantage with GUITAR-Fc, as both enzymatic and nanoparticle-based electrodes suffer from long-term storage. Enzyme-based sensors, while often producing better LODs than GUITAR-Fc, have poor storage stability as horseradish peroxidase degrades after only a few months [4,59]. Similarly, metal nanoparticles show poor storage stability, showing an average loss of 6.1 % over a 2-week period of storage [60-62].

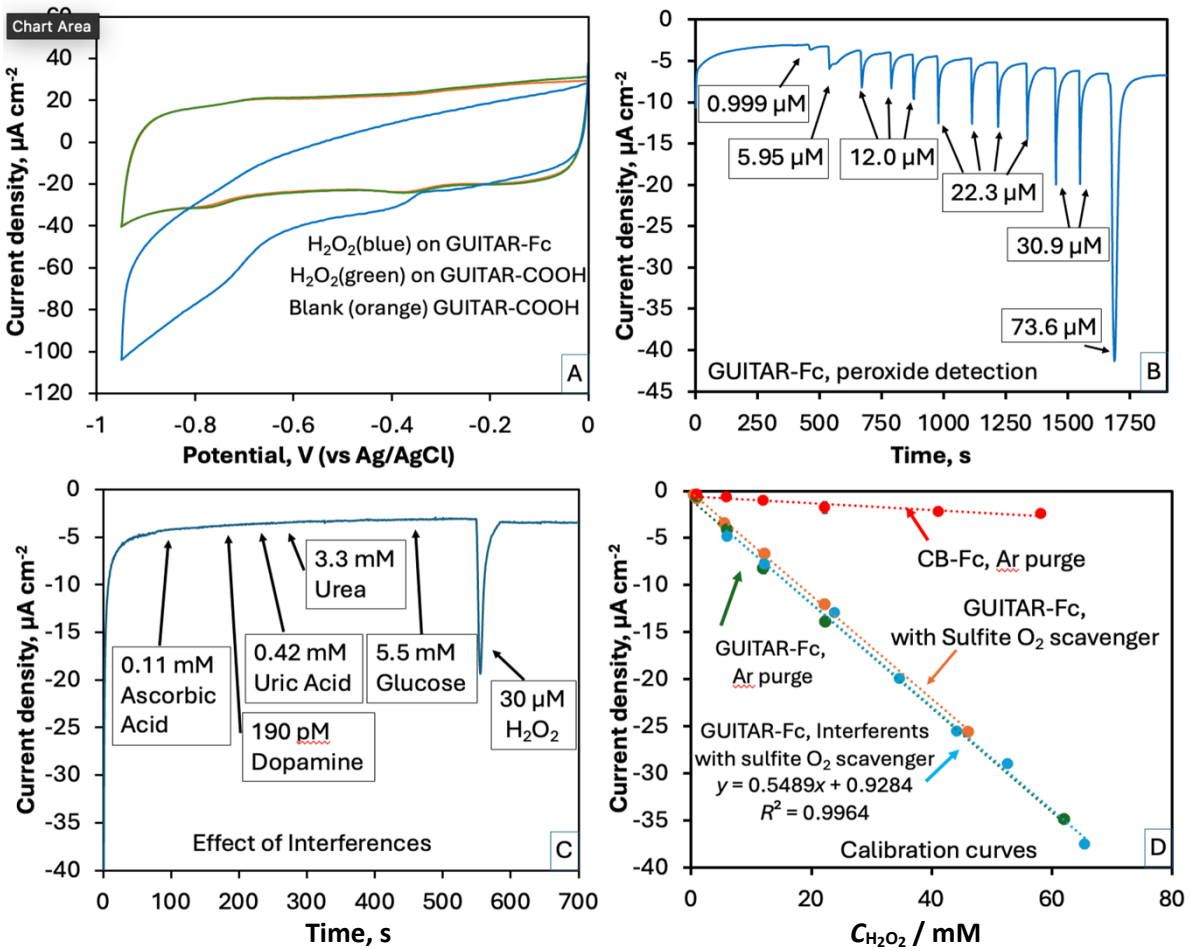

Figure 6. *(A) Cyclic voltammagrams of 60 µM H_2O_2 in 0.1 M phosphate buffer, pH 7.0 at 50 mV s^{-1}. The green CV was a GUITAR-COOH electrode in the presence of 6612 µM H_2O_2, The blue CV was the response with Fc attached. (B) The amperometric response at -0.6 V* vs. *Ag/AgCl for GUITAR-Fc with H_2O_2. (C) Individual responses of interferents at biological concentrations at -0.6 V. (D) The calibration curves from Panel B. GUITAR-Fc shows identical responses for H_2O_2 under Ar purged (green) and in the presence of $O_{2(aq)}$ with 0.009 M Na_2SO_3 (orange). The addition of interferents did not affect the detection of H_2O_2 (blue line) with 0.009 M Na_2SO_3 O_2 scavenger*

The response of the GUITAR-Fc H_2O_2 sensor is free of the common biological interferences. These were examined at the maximum concentrations found in biofluids of interest (interstitial fluid or serum) [7-11]. No current response (Figure 6C) was found for glucose (5.5 mM), ascorbate (100 mM), urea (7 mM), uric acid (0.4 mM), dopamine (200 pM), or $MgCl_2$ (1.1 mM). A full calibration curve was performed in their presence and is overlayed with the previous studies in the absence of interferents (Figure 6D). There is no significant difference between the curves. This can be attributed to the ability to operate the electrochemical sensor using a reductive process, avoiding the electrochemically oxidizable interferents. However, this potential region (-0.6 V *vs.* Ag/AgCl), introduces the interferent of dissolved O_2 (equation (3)). While biological fluids (serum and interstitial fluid) are generally free of dissolved oxygen due to uric and ascorbic acids, this may become a concern over long periods of *ex-vivo* storage. A simple solution is $O_{2(aq)}$ removal from the cell by inert gas purging (Ar) or the addition of low amounts of sodium sulphite as an oxygen scavenger (Equation (4); concentration of 0.009 M Na_2SO_3). Either method gave the same calibration curve for H_2O_2 as shown in Figure 6D.

Table 1. *Literature comparison for ferrocene-based hydrogen peroxide detection*

Linear range, µM	LOD, µM	Sensitivity, µA mM^{-1} m^{-2}	Interference from ascorbate, urea, urate, dopamine, glucose*	Ref.
GUITAR-Fc				
0.45-74	0.34[a], 0.070[b]	553.2	No	This work
Fc redox polymers				
0.08-15	0.08	0.034**	Yes	[63]
0-120	N/R	13.1	N/R	[64]
0-50	0.08	6.884	Yes	[16]
10-10000	2.07	0.05	No	[55]
Fc immobilized particles				
1-1000	0.49	136.4	Yes	[65]
20-4000	5	0.42**	N/R	[20]
Adsorbed or covalently attached Fc				
10-400	0.66	71.4	No	[21]
5-500, 500-4800	5	N/R	N/R	[66]
N/R	50	1.545**	Yes	[22]

*see Figure 6c; **µA mM^{-1}; N/R - not reported; [a]expressed using Equation (6), standard deviation of lowest concentration signal; [b]expressed using the standard deviation of the blank

Conclusions

In this study, we demonstrate the advantages of using the peroxidase-like activity of immobilized Fc for the electrochemical sensing of H_2O_2 (Equation (2)). GUITAR was modified by spontaneous chemical reduction with an *in situ* generated 4-carboxybenzene diazonium chloride, producing carboxylated GUITAR, GUITAR-COOH. This material shows the highest chemical diazonium graft surface density in the literature [39-47]. Carboxylated GUITAR was coupled with aminoferrocene using an amide bond. The system demonstrates a stable, durable bond to the aminoferrocene centre, surviving 50 CV cycles in an aqueous environment with no loss in observed peak currents (Figure 4C). The resulting sensor shows peroxidase-like catalysis for H_2O_2 reduction at -0.6V. This scheme has the best combination of LOD and sensitivity, without the effects of common interferents in biological matrices (Table 1). The demonstrated durability and activity of the GUITAR-supported ferrocene shows great promise for use in other sensing and electrocatalytic schemes.

References

[1] N. Yang, W. Xiao, X. Song, W. Wang, X. Dong, Recent Advances in Tumor Microenvironment Hydrogen Peroxide-Responsive Materials for Cancer Photodynamic Therapy, *Nano-Micro Letters* **12** (2020) 15. https://doi.org/10.1007/s40820-019-0347-0

[2] T. Ali, D. Li, T. N. F. Ponnamperumage, A. K. Peterson, J. Pandey, K. Fatima, J. Brzezinski, J. A. R. Jakusz, H. Gao, G. E. Koelsch, D. S. Murugan, X. Peng, Generation of Hydrogen Peroxide in Cancer Cells: Advancing Therapeutic Approaches for Cancer Treatment, *Cancers* **16** (2024) 2171. https://doi.org/10.3390/cancers16122171

[3] K. Dhara, D. R. Mahapatra, Recent advances in electrochemical nonenzymatic hydrogen peroxide sensors based on nanomaterials: a review, *Journal of Materials Science* **54** (2019) 12319-12357. https://doi.org/10.1007/s10853-019-03750-y

[4] G. I. Berglund, G. H. Carlsson, A. T. Smith, H. Szöke, A. Henriksen, J. Hajdu, The catalytic pathway of horseradish peroxidase at high resolution, *Nature* **417** (2002) 463-468. https://doi.org/10.1038/417463a

[5] C. Yang, M. E. Denno, P. Pyakurel, B. J. Venton, Recent trends in carbon nanomaterial-based electrochemical sensors for biomolecules: A review, *Analytica Chimica Acta* **887** (2015) 17-37. https://doi.org/10.1016/j.aca.2015.05.049

[6] X. Xu, S. Liu, H. Ju, A Novel Hydrogen Peroxide Sensor via the Direct Electrochemistry of Horseradish Peroxidase Immobilized on Colloidal Gold Modified Screen-printed Electrode, *Sensors* **3** (2003) 350-360. https://doi.org/10.3390/s30900350
[7] S. M. Lewis, S. R. Dirksen, M. M. Heitkemper, L. Bucher, M. Harding, *Medical-surgical nursing: assessment and management of clinical problems*, 9th ed., Mosby, St. Louis, Missouri, 2013. https://www.zu.edu.jo/UploadFile/Library/E_Books/Files/LibraryFile_16951_48.pdf
[8] H. R. Bhoot, U. M. Zamwar, S. Chakole, A. Anjankar, Dietary Sources, Bioavailability, and Functions of Ascorbic Acid (Vitamin C) and Its Role in the Common Cold, Tissue Healing, and Iron Metabolism, *Cureus* **15** (11) (2023) e49308. https://doi.org/10.7759/cureus.49308
.[9] L. Goldman, A. I Schafer, *Goldman's Cecil Medicine 24Ed International edition*, Saunders, Philadelphia, United States of America, 2012, p.1470-1475 https://doi.org/10.1016/B978-1-4377-1604-7.00235-9
[10] MedlinePlus, https://medlineplus.gov/ency/article/003487.htm (6/19/2025).
[11] R. Gaikwad, P.R. Thangaraj, A.K. Sen, Direct and rapid measurement of hydrogen peroxide in human blood using a microfluidic device, *Scientific Reports* **11** (2021) 2960. https://doi.org/10.1038/s41598-021-82623-4
[12] R. N. Pittman, Regulation of Tissue Oxygenation, *Colloquium Series on Integrated Systems Physiology: From Molecule to Function* **3** (2011) 1-100. https://doi.org/10.4199/C00029ED1V01Y201103ISP017
[13] A. J. Bard, L. R. Faulkner, H. S. White, *Electrochemical Methods: Fundamentals and Applications*, 3rd ed., John Wiley & Sons, INC., Danvers, United States of America, 2022. ISBN 978-1-119-33405-7
[14] K. H. Rashid, A. A. Khadom, Sodium sulfite as an oxygen scavenger for the corrosion control of mild steel in petroleum refinery wastewater: optimization, mathematical modeling, surface morphology and reaction kinetics studies, *Reaction Kinetics, Mechanisms and Catalysis* **129** (2020) 1027-1046. https://doi.org/10.1007/s11144-020-01738-3
[15] Sariga, A. Varghese, The Renaissance of Ferrocene-Based Electrocatalysts: Properties, Synthesis Strategies, and Applications, *Topics in Current Chemistry* **381** (2023) 32. https://doi.org/10.1007/s41061-023-00441-w
[16] Q. Hu, Y. Fang, X. Yu, J. Huang, L. Wang, A ferrocene-linked metal-covalent organic polymer as a peroxidase-enzyme mimic for dual channel detection of hydrogen peroxide, *The Analyst* **146** (2021) 487-494. https://doi.org/10.1039/D0AN01837F
[17] A. Singh, D.R. Chowdhury, A. Paul, A kinetic study of ferrocenium cation decomposition utilizing an integrated electrochemical methodology composed of cyclic voltammetry and amperometry, *The Analyst* **139** (2014) 5747-5754. https://doi.org/10.1039/C4AN01325E
[18] G. Zotti, G. Schiavon, S. Zecchin, D. Favretto, Dioxygen-decomposition of ferrocenium molecules in acetonitrile: The nat,ure of the electrode-fouling films during ferrocene electrochemistry, *Journal of Electroanalytical Chemistry* **456** (1998) 217-221. https://doi.org/10.1016/S0022-0728(98)00279-4
[19] R. Gracia, D. Mecerreyes, Polymers with redox properties: materials for batteries, biosensors and more, *Polymer Chemistry* **4** (2013) 2206. https://doi.org/10.1039/c3py21118e
[20] V. S. Tripathi, V. B. Kandimalla, H. Ju, Amperometric biosensor for hydrogen peroxide based on ferrocene-bovine serum albumin and multiwall carbon nanotube modified ormosil composite, *Biosensors and Bioelectronics* **21** (2006) 1529-1535. https://doi.org/10.1016/j.bios.2005.07.006
[21] N. A. Ertas, E. Kavak, F. Salman, H. C. Kazici, H. Kivrak, A. Kivrak, Synthesis of Ferrocene Based Naphthoquinones and its Application as Novel Non-enzymatic Hydrogen Peroxide, *Electroanalysis* **32** (2020) 1178-1185. https://doi.org/10.1002/elan.201900715

[22] G.-C. Zhao, M.-Q. Xu, Q. Zhang, A novel hydrogen peroxide sensor based on the redox of ferrocene on room temperature ionic liquid film, *Electrochemistry Communications* **10** (2008) 1924-1926. https://doi.org/10.1016/j.elecom.2008.10.005

[23] H. Kabir, H. Zhu, J. May, K. Hamal, Y. Kan, T. Williams, E. Echeverria, D. N. McIlroy, D. Estrada, P. H. Davis, T. Pandhi, K. Yocham, K. Higginbotham, A. Clearfield, I.F. Cheng, The sp2-sp3 carbon hybridization content of nanocrystalline graphite from pyrolyzed vegetable oil, comparison of electrochemistry and physical properties with other carbon forms and allotropes, *Carbon* **144** (2019) 831-840. https://doi.org/10.1016/j.carbon.2018.12.058

[24] H. Lim, J.S. Lee, H.-J. Shin, H. S. Shin, H. C. Choi, Spatially Resolved Spontaneous Reactivity of Diazonium Salt on Edge and Basal Plane of Graphene without Surfactant and Its Doping Effect, *Langmuir* **26** (2010) 12278-12284. https://doi.org/10.1021/la101254k

[25] J. Greenwood, T. H. Phan, Y. Fujita, Z. Li, O. Ivasenko, W. Vanderlinden, H. Van Gorp, W. Frederickx, G. Lu, K. Tahara, Y. Tobe, H. Uji-i, S.F.L. Mertens, S. De Feyter, Covalent Modification of Graphene and Graphite Using Diazonium Chemistry: Tunable Grafting and Nanomanipulation, *ACS Nano* **9** (2015) 5520-5535. https://doi.org/10.1021/acsnano.5b01580

[26] J. E. Johns, M. C. Hersam, Atomic Covalent Functionalization of Graphene, *Accounts of Chemical Research* **46** (2013) 77-86. https://doi.org/10.1021/ar300143e

[27] B. D. L. Campéon, M. Akada, M. S. Ahmad, Y. Nishikawa, K. Gotoh, Y. Nishina, Non-destructive, uniform, and scalable electrochemical functionalization and exfoliation of graphite, *Carbon* **158** (2020) 356-363. https://doi.org/10.1016/j.carbon.2019.10.085

[28] Y. Wang, C. Li, H. Meng, Y. Lu, H. Fan, Production of functionalized graphitic carbon materials via solvent-free mechanochemical method for supercapacitors and water treatment, *Diamond and Related Materials* **127** (2022) 109193. https://doi.org/10.1016/j.diamond.2022.109193

[29] D. Koirala, F. Dalbec, J. May, K. Hamal, P. B. Allen, F. I. Cheng, Biosensing with Polymerase Chain Reaction-Stable DNA-Functionalized Magnetically Susceptible Carbon-Iron Microparticles, *Analytical Chemistry* **95** (2023) 16631-16638. https://doi.org/10.1021/acs.analchem.3c02978.s001

[30] J. May, D. Koirala, F. Dalbec, J. Russell, H. Xiong, E. Echeverria, D. N. McIlroy, I. F. Cheng, Superhydrophilicity and Antifouling Behavior in Electrochemically Oxidized Nanocrystalline Pseudographite, *Industrial & Engineering Chemistry Research* **62** (2023) 6687-6696. https://doi.org/10.1021/acs.iecr.3c00140

[31] K. Hamal, J. May, D. Koirala, H. Zhu, H. Kabir, E. Echeverria, D.N. McIlroy, N. Nicholas, I.F. Cheng, Highly Stable, Low-Cost Metal-Free Oxygen Reduction Reaction Electrocatalyst Based on Nitrogen-Doped Pseudo-Graphite, *Energy & Fuels* **35** (2021) 10146-10155. https://doi.org/10.1021/acs.energyfuels.1c00658

[32] K. Hamal, D. Koirala, J. May, F. Dalbec, N. Nicholas, I. F. Cheng, An oxygen reduction reaction electrocatalyst tuned for hydrogen peroxide generation based on a pseudo-graphite doped with graphitic nitrogen, *Journal of Electrochemical Science and Engineering* **12** (2022) 1009-1023. https://doi.org/10.5599/jese.1407

[33] M. A. Isaacs, J. Davies-Jones, P.R. Davies, S. Guan, R. Lee, D. J. Morgan, R. Palgrave, Advanced XPS characterization: XPS-based multi-technique analyses for comprehensive understanding of functional materials, *Materials Chemistry Frontiers* **5** (2021) 7931-7963. https://doi.org/10.1039/D1QM00969A

[34] S. Tougaard, Improved XPS analysis by visual inspection of the survey spectrum, *Surface and Interface Analysis* **50** (2018) 657-666. https://doi.org/10.1002/sia.6456

[35] C. D. Wagner, Sensitivity factors for XPS analysis of surface atoms, *Journal of Electron Spectroscopy and Related Phenomena*. **32** (1983) 99-102 https://doi.org/10.1016/0368-2048(83)85087-7

[36] The International XPS Database of Monochromatic XPS Reference Spectra, Peak-fits, & Six B. E. Tables, https://xpsdatabase.net/carbon-spectra-graphene-fresh-peel-from-hopg (6/19/2025)
[37] X-ray Photoelectron Spectroscopy (XPS) Reference Pages, https://www.xpsfitting.com/2022/06/graphiticgraphenecarbon-nanotube-c-1s.html (6/19/2025).
[38] ThermoFischer Scientific, https://www.thermofisher.com/us/en/home/materials-science/learning-center/periodic-table/non-metal/carbon.html (6/19/2025).
[39] M. Toupin, D. Bélanger, Thermal Stability Study of Aryl Modified Carbon Black by in Situ Generated Diazonium Salt, *The Journal of Physical Chemistry C* **111** (2007) 5394-5401 https://doi.org/10.1021/jp066868e
[40] M. Toupin, D. Bélanger, Spontaneous Functionalization of Carbon Black by Reaction with 4-Nitrophenyldiazonium Cations, *Langmuir* **24** (2008) 1910-1917. https://doi.org/10.1021/la702556n
[41] G. Pognon, T. Brousse, L. Demarconnay, D. Bélanger, Performance and stability of electrochemical capacitor based on anthraquinone modified activated carbon, *Journal of Power Sources* **196** (2011) 4117-4122. https://doi.org/10.1016/j.jpowsour.2010.09.097
[42] G. Pognon, C. Cougnon, D. Mayilukila, D. Bélanger, Catechol-Modified Activated Carbon Prepared by the Diazonium Chemistry for Application as Active Electrode Material in Electrochemical Capacitor, *ACS Applied Materials & Interfaces* **4** (2012) 3788-3796. https://doi.org/10.1021/am301284n
[43] E. Lebègue, T. Brousse, J. Gaubicher, C. Cougnon, Spontaneous arylation of activated carbon from aminobenzene organic acids as source of diazonium ions in mild conditions, *Electrochimica Acta* **88** (2013) 680-687. https://doi.org/10.1016/j.electacta.2012.10.132
[44] E. Lebègue, L. Madec, T. Brousse, J. Gaubicher, E. Levillain, C. Cougnon, Modification of activated carbons based on diazonium ions in situ produced from aminobenzene organic acid without addition of other acid, *Journal of Materials Chemistry* **21** (2011) 12221. https://doi.org/10.1039/c1jm11538c
[45] J. A. Belmont, Process for preparing carbon materials with diazonium salts and resultant carbon products, US5554739A, 1994. https://patents.google.com/patent/US5554739A/en
[46] P. Salice, E. Fabris, C. Sartorio, D. Fenaroli, V. Figà, M. P. Casaletto, S. Cataldo, B. Pignataro, E. Menna, An insight into the functionalisation of carbon nanotubes by diazonium chemistry: Towards a controlled decoration, *Carbon* **74** (2014) 73-82. https://doi.org/10.1016/j.carbon.2014.02.084
[47] J. L. Bahr, J. M. Tour, Highly Functionalized Carbon Nanotubes Using in Situ Generated Diazonium Compounds, *Chemistry of Materials* **13** (2001) 3823-3824. https://doi.org/10.1021/cm0109903
[48] X-ray Photoelectron Spectroscopy (XPS) Reference Pages, www.xpsfitting.com (6/19/2025).
[49] J. Gomez-Bolivar, I. P. Mikheenko, R. L. Orozco, S. Sharma, D. Banerjee, M. Walker, R. A. Hand, M. L. Merroun, L. E. Macaskie, Synthesis of Pd/Ru Bimetallic Nanoparticles by Escherichia coli and Potential as a Catalyst for Upgrading 5-Hydroxymethyl Furfural Into Liquid Fuel Precursors, *Frontiers in Microbiology* **10** (2019) 1276. https://doi.org/10.3389/fmicb.2019.01276
[50] L. H. Grey, H.-Y. Nie, M. C. Biesinger, Defining the nature of adventitious carbon and improving its merit as a charge correction reference for XPS, *Applied Surface Science* **653** (2024) 159319. https://doi.org/10.1016/j.apsusc.2024.159319
[51] J. Pinson, F. Podvorica, Attachment of organic layers to conductive or semiconductive surfaces by reduction of diazonium salts, *Chemical Society Reviews* **34** (2005) 429. https://doi.org/10.1039/b406228k

[52] A. Mattiuzzi, Q. Lenne, J. Carvalho Padilha, L. Troian-Gautier, Y. R. Leroux, I. Jabin, C. Lagrost, Strategies for the Formation of Monolayers from Diazonium Salts: Unconventional Grafting Media, Unconventional Building Blocks, *Frontiers in Chemistry* **8** (2020) 559. https://doi.org/10.3389/fchem.2020.00559
[53] C. Gautier, I. López, T. Breton, A post-functionalization toolbox for diazonium (electro)-grafted surfaces: review of the coupling methods, *Materials Advances* **2** (2021) 2773-2810. https://doi.org/10.1039/D1MA00077B
[54] R.G. Compton, C.E. Banks, *Understanding Voltammetry*, 2nd ed., Imperial College Press, London, 2011. https://doi.org/10.1142/p726
[55] M. Mattoussi, F. Matoussi, N. Raouafi, Non-enzymatic amperometric sensor for hydrogen peroxide detection based on a ferrocene-containing cross-linked redox-active polymer, *Sensors and Actuators B* **274** (2018) 412-418. https://doi.org/10.1016/j.snb.2018.07.145
[56] E. Theodorsson, Limit of detection, limit of quantification and limit of blank, *European Federation of Clinical Chemistry and Laboratory Medicine*. (n.d.).
[57] *Limit of detection in analysis*, in: The IUPAC Compendium of Chemical Terminology, , International Union of Pure and Applied Chemistry (IUPAC), Research Triangle Park, NC, 2014 https://doi.org/10.1351/goldbook.L03540
[58] F. Allegrini, A. C. Olivieri, *Comprehensive Chemometrics 2nd ed.*, Elsevier, Cambridge, United States of America, 2020, p. 441-463. https://doi.org/10.1016/B978-0-12-409547-2.14612-8
[59] MilliporeSigma,https://www.sigmaaldrich.com/US/en/technical-documents/technical-article/protein-biology/enzyme-activity-assays/peroxidase-enzymes?srsltid=AfmBOoqsKT40Z3ZbHo2kuYlfXI47VdQkzwSoUOA0fAt78sXWpkT60Vq7#horseradish (6/19/2025).
[60] J. Dou, G. Zhu, B. Hu, J. Yang, Y. Ge, X. Li, J. Liu, Wall thickness-tunable AgNPs-NCNTs for hydrogen peroxide sensing and oxygen reduction reaction, *Electrochimica Acta* **306** (2019) 466-476. https://doi.org/10.1016/j.electacta.2019.03.152
[61] W. Hooch Antink, Y. Choi, K. Seong, Y. Piao, Simple synthesis of CuO/Ag nanocomposite electrode using precursor ink for non-enzymatic electrochemical hydrogen peroxide sensing, *Sensors and Actuators B* **255** (2018) 1995-2001. https://doi.org/10.1016/j.snb.2017.08.217
[62] M. Guler, V. Turkoglu, A. Bulut, M. Zahmakiran, Electrochemical sensing of hydrogen peroxide using Pd@Ag bimetallic nanoparticles decorated functionalized reduced graphene oxide, *Electrochimica Acta* **263** (2018) 118-126. https://doi.org/10.1016/j.electacta.2018.01.048
[63] A. Mulchandani, S. Pan, Ferrocene-Conjugatedm-Phenylenediamine Conducting Polymer-Incorporated Peroxidase Biosensors, *Analytical Biochemistry* **267** (1999) 141-147. https://doi.org/10.1006/abio.1998.2983
[64] H. Zhang, H. Hu, Y. Li, J. Wang, L. Ma, A ferrocene-based hydrogel as flexible electrochemical biosensor for oxidative stress detection and antioxidation treatment, *Biosensors and Bioelectronics* **248** (2024) 115997. https://doi.org/10.1016/j.bios.2023.115997
[65] B. Wu, S. Yeasmin, Y. Liu, L.-J. Cheng, Ferrocene-grafted carbon nanotubes for sensitive non-enzymatic electrochemical detection of hydrogen peroxide, *Journal of Electroanalytical Chemistry* **908** (2022) 116101. https://doi.org/10.1016/j.jelechem.2022.116101
[66] N. Sun, L. Guan, Z. Shi, N. Li, Z. Gu, Z. Zhu, M. Li, Y. Shao, Ferrocene Peapod Modified Electrodes: Preparation, Characterization, and Mediation of H_2O_2, *Analytical Chemistry* **78** (2006) 6050-6057. https://doi.org/10.1021/ac060396i